RNA (2002), *8*:110–122. Cambridge University Press. Printed in the USA.

DOI: 10.1017.S1355838201012079

The Brome mosaic virus subgenomic promoter hairpin is structurally similar to the iron-responsive element and functionally equivalent to the minus-strand core promoter stem-loop C

P.C. JOOST HAASNOOT, RENÉ C.L. OLSTHOORN, and JOHN F. BOL
Institute of Molecular Plant Sciences, Gorlaeus Laboratories, Leiden University, 2300 RA Leiden, The Netherlands

ABSTRACT

In the *Bromoviridae* family of plant viruses, trinucleotide hairpin loops play an important role in RNA transcription. Recently, we reported that Brome mosaic virus (BMV) subgenomic (sg) transcription depended on the formation of an unusual triloop hairpin. By native gel electrophoresis, enzymatic structure probing, and NMR spectroscopy it is shown here that in the absence of viral replicase the hexanucleotide loop 5′C_1AUAG_5A3′ of this RNA structure can adopt a pseudo trinucleotide loop conformation by transloop base pairing between C_1 and G_5. By means of in vitro replication assays using partially purified BMV RNA-dependent RNA polymerase (RdRp) it was found that other base pairs contribute to sg transcription, probably by stabilizing the formation of this pseudo triloop, which is proposed to be the primary element recognized by the viral replicase. The BMV pseudo triloop structure strongly resembles iron-responsive elements (IREs) in cellular messenger RNAs and may represent a general protein-binding motif. In addition, in vitro replication assays showed that the BMV sg hairpin is functionally equivalent to the minus-strand core promoter hairpin stem-loop C at the 3′ end of BMV RNAs. Replacement of the sg hairpin by stem-loop C yielded increased sg promoter activity whereas replacement of stem-loop C by the sg hairpin resulted in reduced minus-strand promoter activity. We conclude that AUA triloops represent the common motif in the BMV sg and minus-strand promoters required for recruitment of the viral replicase. Additional sequence elements of the minus-strand promoter are proposed to direct the RdRp to the initiation site at the 3′ end of the genomic RNA.

Keywords: *Bromoviridae*; RNA polymerase; RNA–protein interaction; triloop; viral replication

INTRODUCTION

An essential step in the replication of a virus is the specific interaction of the virally encoded replicase protein(s) with viral promoter sequences. In many positive-strand RNA viruses, RNA secondary structures have been shown to be involved in recruiting the complex of RNA-dependent RNA polymerase (RdRp) and possible host factors to the viral promoter and transcription initiation site (Buck, 1996). The RNA secondary structures involved in minus-strand RNA synthesis are, in most cases, located in the 3′ untranslated region (UTR) of the genomic RNA (Duggal et al., 1994). These structures can be rather complex, such as the tRNA-like structures that have been shown to play a central role in the production of minus-strand RNAs for tymo-, bromo-, cucumo-, and tobamo viruses (Dreher, 1999). For other viruses such as Poliovirus, Hepatitis C virus (HCV), Turnip crinkle virus, and Bamboo mosaic virus, pseudoknots and/or stem-loop structures have been identified as the main targets for the RdRp (Carpenter & Simon, 1998; Tsai et al., 1999; Wang et al., 1999; Oh et al., 2000).

In addition to replication of genomic RNA, the RdRps of viruses from the Alphavirus-like superfamily are also involved in production of subgenomic (sg) RNAs. For the synthesis of sg RNAs, three basic mechanisms have been proposed, involving internal initiation on the viral minus-strand RNA (Miller et al., 1985; van der Kuyl et al., 1990; Wang & Simon, 1997), premature termi-

Reprint requests to: John F. Bol, Gorlaeus Laboratories, Leiden University, PO Box 9502, 2300 RA Leiden, The Netherlands; e-mail: j.bol@chem.leidenuniv.nl.

nation during minus-strand RNA synthesis (Sit et al., 1998), or discontinuous transcription during plus- or minus-strand RNA synthesis (Lai & Cavanagh, 1997; Sawicki & Sawicki, 1998; van Marle et al., 1999). However different these mechanisms are, it is believed that the RNA secondary structure plays a central role in all types of sg RNA synthesis (Miller & Koev, 2000).

Our research is focused on the RNA secondary structures involved in the replication of Alfalfa mosaic virus (AMV) and Brome mosaic virus (BMV), which are both members of the family *Bromoviridae* (Rybicki, 1995). These viruses have a tripartite genome. RNAs 1 and 2 encode the replicase proteins whereas RNA 3 encodes the movement protein and the coat protein (CP), which is translated from the sg messenger RNA 4 (reviewed in Bol, 1999). The promoter sequences for minus-strand production of AMV and BMV have been studied extensively. A tRNA-like structure at the 3′ end of BMV RNAs is required for minus-strand RNA synthesis (Dreher & Hall, 1988). Recently, tRNA-like structures involved in minus-strand RNA synthesis have also been identified in genomic RNAs of AMV and the closely related ilarviruses. The AMV tRNA-like structure has been shown to function as a molecular switch that changes conformation upon binding of CP. This conformational change shuts off minus-strand RNA synthesis (Olsthoorn et al., 1999). In BMV, the triloop AUA of stem-loop C in the 3′ UTR has been identified as the core recognition site for the BMV RdRp (Chapman & Kao, 1999; Kim et al., 2000). Recently, we provided evidence that triloop hairpin structures are also essential for both AMV sg and minus-strand RNA synthesis (Haasnoot et al., 2000; R.C.L. Olsthoorn & J.F. Bol, submitted for publ.). In addition, our data indicated that an AUA triloop hairpin (Fig. 1) is also important for BMV sg transcription (Haasnoot et al., 2000). However, another model has been proposed in which this transcription takes place through sequence-specific contacts with the replicase (Siegel et al., 1997; Adkins & Kao, 1998).

In the current study, we have analyzed the proposed BMV sg hairpin in further detail, using structure probing, native gel electrophoresis, NMR analysis, and in vitro replication assays. We demonstrate that in vitro this hairpin is functionally equivalent to the BMV hairpin stem-loop C in the BMV minus-strand promoter. We show that the AUA triloops of these structures represent the common motif that is required for BMV RdRp recruitment in both sg and minus-strand RNA synthesis. Furthermore, we show that the BMV sg hairpin has many features in common with iron-responsive elements (IREs) and other well-characterized protein-binding RNA structures. Comparison of the loops of these RNA structures suggests that a pseudo triloop that is formed by 5′C_1G_5 transloop base pairing across a hexanucleotide loop is a general RNA motif involved in specific protein binding.

RESULTS

Analysis of the BMV sg hairpin structure by gel electrophoresis and RNase T1 probing

Previously, we have shown that base pairing between nucleotides C-13 and G-17 relative to the sg transcription initiation site +1 is essential for sg transcription in vitro by the BMV RdRp (Fig. 1A; Haasnoot et al., 2000). This CG base pair converts the otherwise hexanucleotide loop 5′C_1AUAG_5A3', by transloop base pairing between the first and fifth nucleotide, into a 5′AUA trinucleotide loop that is followed by a bulged A-residue. This so-called pseudo triloop is expected to have a relatively low stability as the bulged A-residue will hinder the base pairing between C-13 and G-17. We wanted to determine whether formation of the pseudo triloop in the sg hairpin in BMV minus-strand RNA 3 could occur in the absence of purified RdRp or took place only in the presence of RdRp by an induced fit mechanism. Synthetic RNA fragments 14 nt long were made, with sequences corresponding to the wild-type sg hairpin and a mutant in which the transloop CG base pair was mutated into AG (mutant A-13 shown in Fig. 1B). The RNAs were subjected to gel electrophoresis under denaturing and nondenaturing conditions. Under denaturing conditions, the wild-type and A-13 fragments comigrated (Fig. 1C, left panel). However, when electrophoresis was done under native conditions at a physiological temperature (26 °C), the wild-type fragment migrated ahead of mutant A-13 (Fig. 1C, right panel). This suggests that the wild-type fragment has a more compact structure due to formation of the pseudo triloop in the absence of RdRp.

In another approach, we analyzed base pairing in the two RNA fragments by structure probing with RNase T1, which cuts specifically 3′ of single-stranded guanosine residues (Fig. 1B). The 5′-labeled RNA fragments WT and A-13 were treated with increasing concentrations of ribonuclease T1 and the products were separated by denaturing gel electrophoresis. The undigested fragments migrated as double bands in this experiment. In both fragments, only the G-residue in the hexanucleotide loop was accessible to T1 nuclease under the conditions used. At the highest concentration of T1 RNase used, 40% of the wild-type fragment and only 5% of the mutant remained undigested after the incubation (Fig. 1D). This is consistent with the G-residue in the pseudo triloop of the wild-type fragment being partially protected from digestion by base pairing with the C-residue in this loop.

Analysis of the BMV sg hairpin structure by NMR

Base pairing in the BMV sg hairpin was further investigated by one-dimensional imino proton NMR analysis

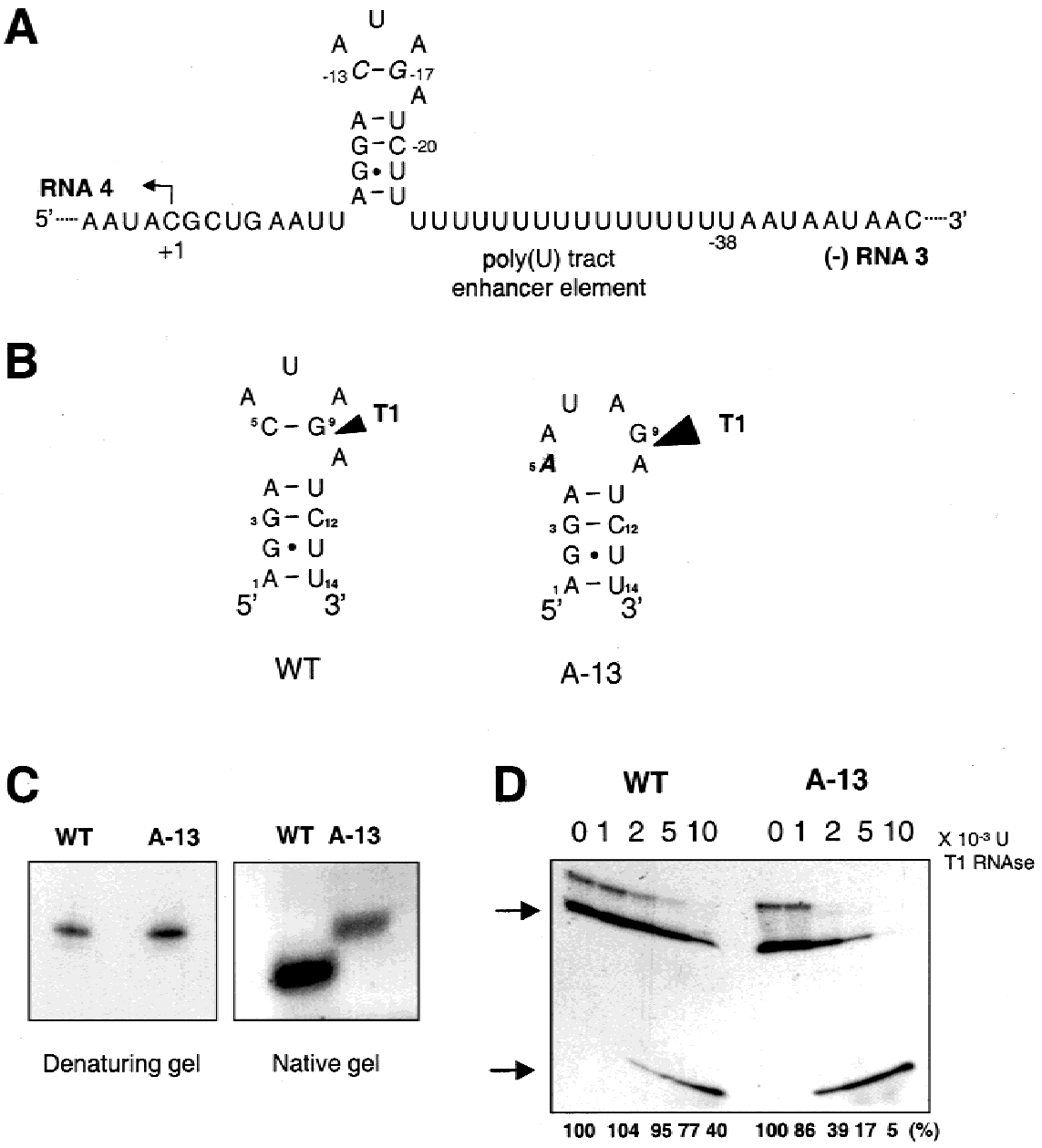

FIGURE 1. Analysis of the pseudo triloop of the BMV sg promoter hairpin using nondenaturing gel electrophoresis and RNase T1 structure probing. **A**: Nucleotide sequence of BMV minus-strand RNA 3 (nt 1196–1247), encompassing the sg core promoter (−20/+1) with the proposed hairpin structure and the poly(U) tract enhancer element. Indicated are the RNA 4 transcription initiation site +1 and the nt C-13 and G-17 which were previously shown to form an essential base pair (Haasnoot et al., 2000). **B**: Predicted base pairing of synthetic oligoribonucleotides corresponding to the wild-type (WT) BMV sg hairpin and a mutant (A-13) with the C-residue of the transloop base pair mutated into an A-residue (indicated in bold). The single cleavage obtained by RNase T1 digestion is indicated by an arrowhead. **C**: Gel electrophoresis of WT and A-13 oligoribonucleotides under denaturing conditions (left panel) and nondenaturing conditions (right panel). **D**: Gel electrophoresis of 5′-terminally labeled WT and A-13 oligoribonucleotides after incubation of the RNAs for 15 min with the indicated amounts of RNase T1. Full-length RNAs and 5′ labeled digestion products are indicated by arrows. The percentage of undigested RNA after incubation is indicated.

of the 14-nt RNA fragments corresponding to the wild-type sg sequence and mutant A-13. Nondenaturing gel electrophoresis showed that RNA fragments WT and A-13 migrated predominantly as monomers (Fig. 1C), which rendered these RNAs suitable for NMR analysis. The wild-type BMV sg hairpin is predicted to show in a one-dimensional NMR spectrum a total of six imino proton resonances that are involved in the five base pairs comprising the stem region (two from the GU pair and three from the GC and two AU base pairs) plus one

imino proton from the transloop 5′CG base pair. The NMR spectrum of mutant A-13 is expected to lack the sixth imino proton resonance due to disruption of the transloop base pair. In accordance with these predictions, the spectrum of the wild-type fragment shows six peaks (Fig. 2, bottom): two peaks left of 13.5 ppm, which are in the typical range of AU base pairs, one peak at 12.7 ppm, which is characteristic for GC base pairs, and three peaks upfield of 12 ppm, which are typical for imino protons of GU pairs or non-hydrogen bonded imino protons from uridine and guanosine residues (Sierzputowska-Gracz et al., 1995). The spectrum of the A-13 mutant (Fig. 2, top) clearly indicates that the C-to-A mutation affects the structure of the RNA fragment. The signals corresponding to the lower two base pairs of the stem (U14, U13, and G2) are reduced, indicating that the stability of the stem was lowered by the mutation. As predicted, the peak corresponding to the transloop imino proton G9 (arrow in Fig. 2) is drastically affected. Although two-dimensional NMR spectroscopy would be required for unambiguous assignment of the peaks, the results are in agreement with the proposed base pairing in the BMV sg hairpin and with the conclusion from the gel electrophoretic analysis and structure probing experiments that the transloop base pair affects the structure of the RNA fragment. Together, these data support the notion that the transloop 5′C_1G_5 base pair is able to form in the absence of RdRp and that recognition of the sg promoter by the RdRp is likely to involve the intact AUA pseudo triloop.

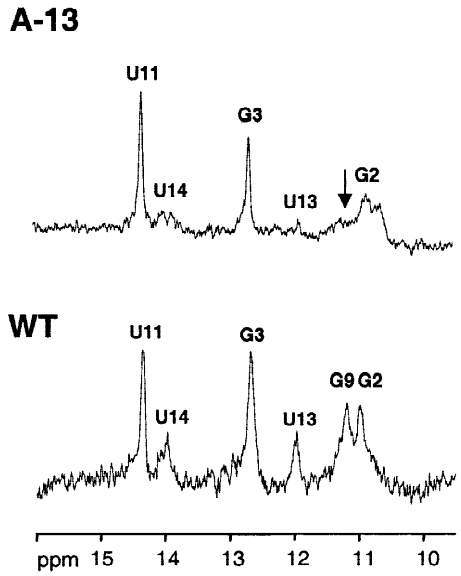

FIGURE 2. Analysis of base pairing in the BMV sg hairpin by NMR spectroscopy. One-dimensional imino proton NMR spectra of the WT and A-13 oligoribonucleotides shown in Figure 1B. Assignment of peaks to nucleotides numbered in Figure 1B is indicated. The arrow indicates the position of the G9 imino proton.

Mutational analysis of the stem of the BMV sg hairpin

Several mutations were engineered in the stem region of the BMV sg hairpin to determine the role of the primary and secondary structure of this region in sg promoter activity. Mutant transcripts obtained by transcription of PCR fragments with T7 RNA polymerase were used as templates for partially purified BMV RdRp in an in vitro assay. The transcripts (shown in Fig. 3A) contained a 25-nt promoter sequence (numbered −1 to −25) 3′ of the transcription start site (taken as +1) and a 5′ template sequence of 19 nt. Previously, we showed that disruption of the transloop 5′CG base pair (nt −13/−17) and thus disruption of the pseudo triloop, abolished sg promoter activity, whereas reversion of this base pair into G-13/C-17 restored activity to about 20% of wild type (Haasnoot et al., 2000). Figure 3 shows that disruption of one of the three base pairs below the bulged A-residue had less dramatic effects on sg pro-

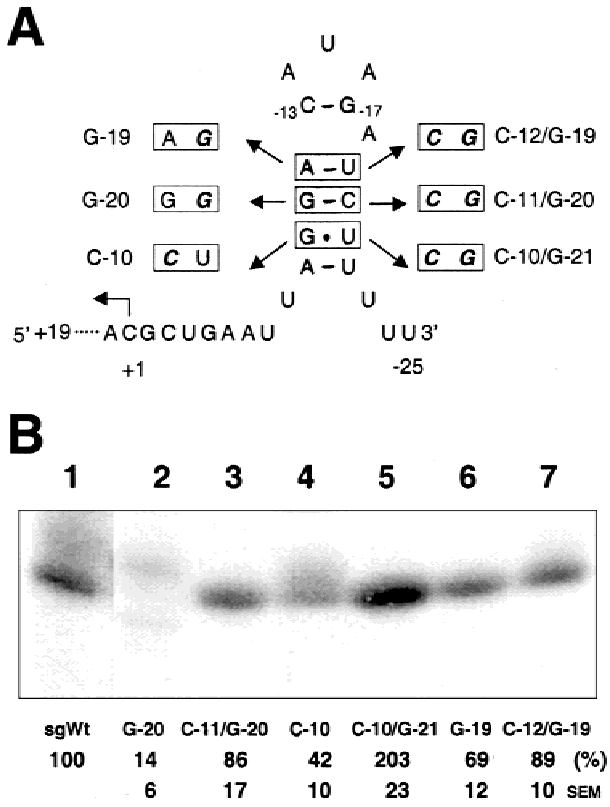

FIGURE 3. Mutational analysis of the stem of the BMV sg hairpin. **A**: Predicted secondary structure of nt −25 to +1 of the wild-type sg promoter (sgWt); the sequence of nt +2 to +19 in the template transcript is not given. Mutations introduced in the stem of the sg hairpin are indicated in bold italics and the names of the mutants are given. **B**: Gel electrophoretic analysis of RNA products synthesized by the RdRp in in vitro assays with the template RNAs shown in **A**. The relative activity levels at the bottom of the panel represent the average of three independent experiments; template activity of sgWt was taken as 100%. The standard error of the mean (SEM) is indicated.

moter activity. Disruption of the AU base pair −12/−19 (mutant G-19) resulted in 69% activity, whereas replacement by a CG base pair (mutant C-12/G-19) resulted in 89% activity. Apparently, this base pair is not critical for promoter activity. Disruption of the GC base pair −11/−20 (mutant G-20) or its reversion into CG (mutant C-11/G-20) resulted in activities of 14% and 86%, respectively, indicating that this base pair contributes to promoter activity. Mutation of the GU pair −10/−21 into a CU mismatch (mutant C-10) reduced activity to 42%, whereas replacement by a CG base pair (mutant C-10/G-21) increased activity to 203% of the wild-type promoter activity. Apparently, also at this position base pairing contributes to promoter activity.

Stem-loop C from the BMV minus-strand promoter has sg promoter activity

In addition to the BMV sg core promoter (nt −20 to +1), additional upstream enhancer elements are required to obtain full sg transcription in vitro and in vivo. The first upstream element that acts as an enhancer for the BMV sg transcription is the poly(U) tract at position −21 to −38 (see Fig. 1A; French & Ahlquist, 1987; Marsh et al., 1988; Adkins et al., 1997). Deletion of this poly(U) tract dramatically reduced RNA 4 synthesis in vivo (French & Ahlquist, 1988; Smirnyagina et al., 1994). However, after passaging a BMV mutant in which this poly(U) stretch was deleted, Smirnyagina et al. (1994) isolated several revertants. One of these revertants contained a second site mutation in the sg core promoter, changing nucleotide A-18 to U. This mutation restored sg promoter activity to 35% of that of the wild type. We noticed that the core promoter of this revertant could be folded into the hairpin structure shown in Figure 4A (panel sgR), in which the wild-type pseudo triloop is reverted to a normal AUA triloop that lacks the bulged A-residue of the wild-type promoter (Fig. 4A, panel sgWt). In addition, we noticed that this hairpin resembled stem-loop C in the tRNA-like structure at the 3′ end of plus-strand BMV RNA 3 (see boxed sequence in Figure 5A). Stem-loop C has been shown to function as the minus-strand core promoter and RdRp recognition site in vitro (Dreher & Hall, 1988; Chapman & Kao, 1999; Kim et al., 2000). Moreover, for both the sg hairpin and stem-loop C it has been shown that only the 5′ A in the AUA loop is required for transcription in a sequence-specific manner (Rao & Hall, 1993; Siegel et al., 1997; Chapman & Kao, 1999; Kim et al., 2000).

These features indicate that the sg hairpin and stem-loop C may fulfil similar functions in recognition of the sg promoter and minus-strand promoter by the viral RdRp. To test this hypothesis, we measured the template activity of chimeric sg promoters in which the sg hairpin was replaced by either the revertant sg hairpin (sgR) or stem-loop C (sgC; Fig. 4A). The wild-type sg promoter template (nt −25 to +19) was used as a

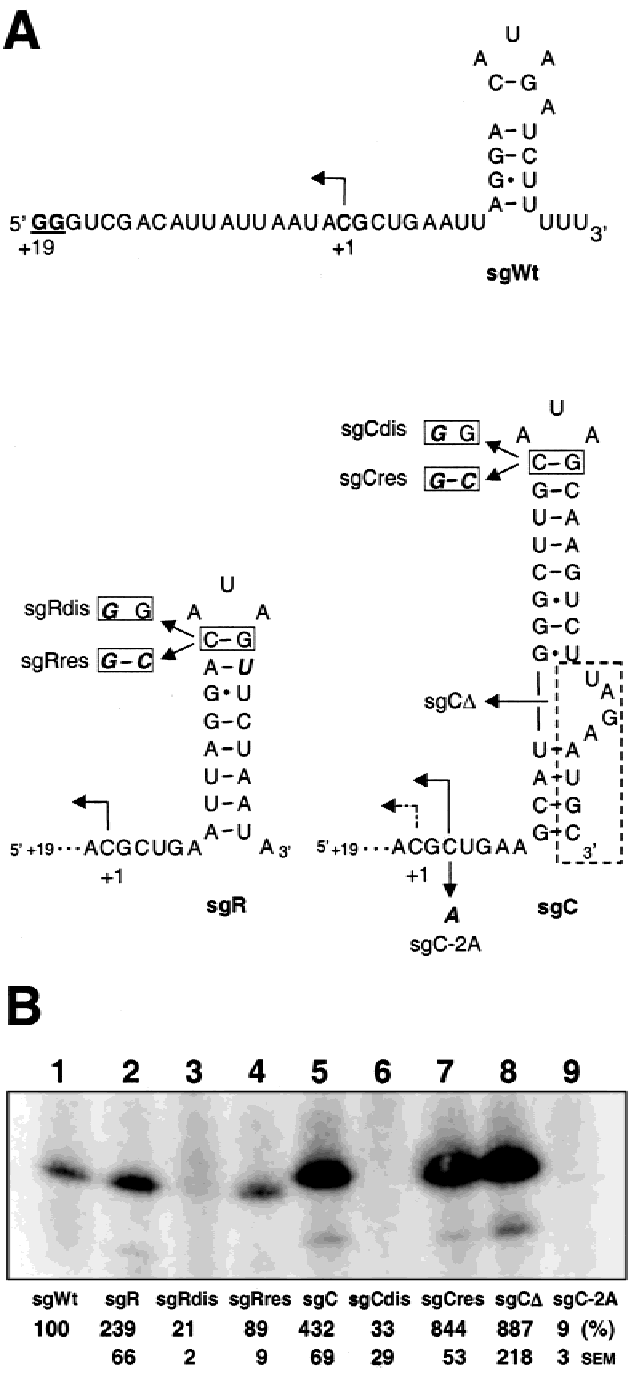

FIGURE 4. Functional equivalence of the wild-type sg hairpin, the hairpin of a second-site revertant generated by a BMV mutant in planta and the stem-loop C hairpin from the BMV minus-strand promoter. **A**: Predicted secondary structure of the wild-type sg promoter (sgWt) and chimeric sg promoters with the sg hairpin replaced by the revertant hairpin (sgR) or stem-loop C hairpin (sgC). In the revertant, the bulged A of the wild type is mutated to a U-residue (bold italic) and the poly(U) track is deleted. Mutations introduced in sgR and sgC are indicated. The bold underlined nucleotides (+18 and +19) are derived from the T7 promoter. **B**: Gel electrophoretic analysis of RNA products synthesized by the RdRp in in vitro assays with the template RNAs shown in **A**. The relative activity levels at the bottom of the panel represent the average of three independent experiments; template activity of sgWt was taken as 100%. The standard error of the mean (SEM) is indicated.

control. The three constructs are shown in Figure 4A. Mutant sgR differed from the sgWt construct by having a U-residue at the position of A-18 and by replacement of the 3′ terminal four U-residues by the sequence 5′AAUA. This sequence flanks the 3′ end of the poly(U) track that is deleted in the revertant. In mutant sgC, stem-loop C was fused to sequences corresponding to nt −6 to +19 from the sgWt construct. All constructs contained a template sequence of 19 nt downstream of the C-residue marked with the hooked arrow and were expected to direct synthesis of RNA products of similar size. In an in vitro RdRp assay, sgR directed the synthesis of a product of wild-type length but promoter activity was two to three times higher than the activity of the wild-type sg promoter (Fig. 4B, lane 2). This indicates that also in vitro the substitution of A-18 to U in sgR mimics the enhancing effect of the poly-U tract. To test whether the observed promoter activity of sgR was dependent on the formation of the trinucleotide AUA loop, mutant sgRdis was constructed in which the loop closing CG base pair is disrupted by mutation to GG (Fig. 4A). This mutation resulted in a decrease of transcription to 21%, which was restored to 89% by introducing the compensatory mutation sgRres (Fig. 4B, lanes 3 and 4). Apparently the triloop AUA of the revertant and the pseudo triloop of the wild-type sg promoter are recognized by the RdRp in a similar way.

The activity of the sgC construct was four to five times higher than the wild-type sg promoter activity (Fig. 4B, lane 5). Disruption of the closing CG base pair in mutant sgCdis resulted in a decrease of template activity to 33% (Fig. 4B, lane 6). A compensatory mutation in mutant sgCres reversed the CG base pair into GC and fully restored template activity (Fig. 4B, lane 7). This showed that also in the sgC promoter the formation of the AUA triloop was essential for recognition by the RdRp. The product synthesized under the control of the sgC construct migrated more slowly than the wild-type product (Fig. 4B, lane 5), suggesting that an alternative site was used for initiation. Deletion of the 3′ terminal 8 nt of this chimeric promoter (boxed region in Fig. 4A; mutant sgCΔ) did not affect promoter activity or the size of the transcript (Fig. 4B, lane 8). When the C-residue in sgC that corresponds to the C-residue at position −2 in the wild-type sg promoter was mutated into an A-residue (mutant sgC-2A; Fig. 4A), template activity of the construct was virtually abolished (Fig. 4B,

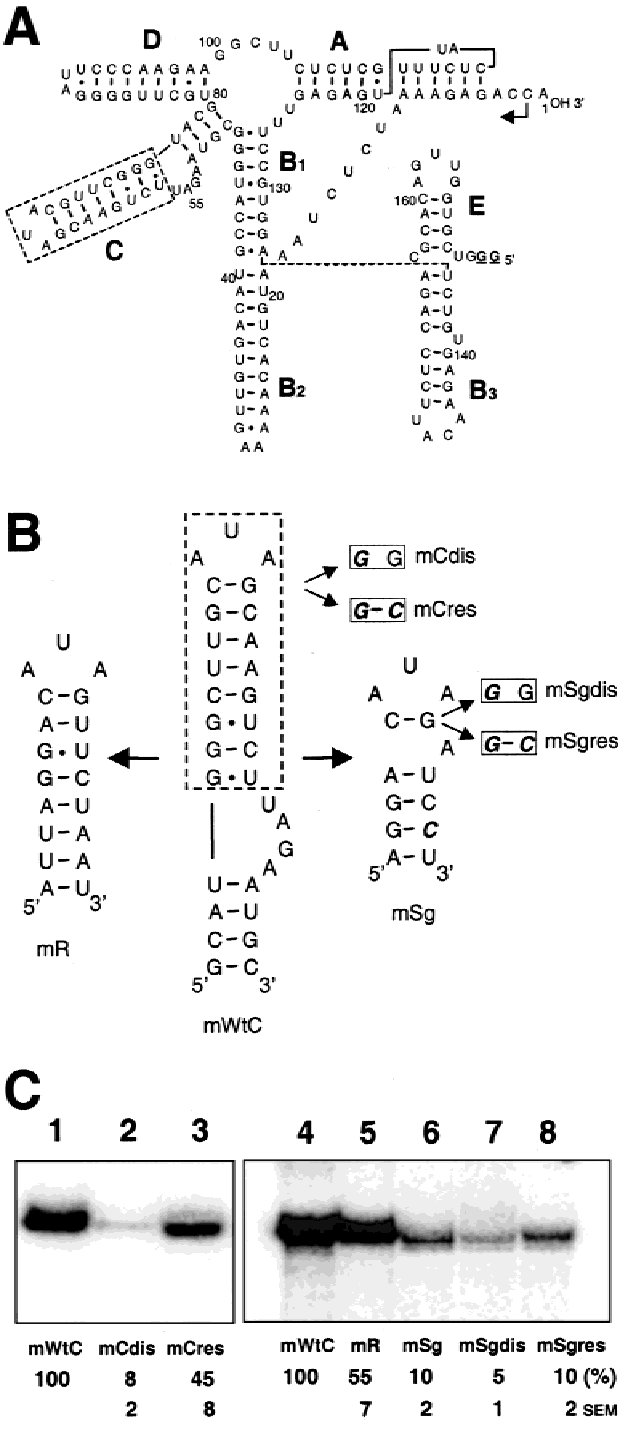

FIGURE 5. Functional equivalence of the stem-loop C hairpin and sg hairpin in BMV minus-strand promoter activity. **A**: Predicted secondary structure of an RNA transcript corresponding to the 3′ terminal 173 nt of plus-strand BMV RNA 3. Stem-loop structures A to E are indicated; note that stem-loop A is involved in a pseudoknot interaction. Mutations shown in Figure 5B were introduced in the boxed region of stem-loop C. The start site of minus-strand RNA synthesis used by the BMV RdRp is indicated by an arrow. The 5′ terminal 2 nt (bold and underlined) are derived from the T7 promoter. **B**: Predicted secondary structure of the stem-loop C hairpin in template transcripts corresponding to the 3′ terminal 173 nt of BMV RNA 3 (mWtC) and mutants in which the stem-loop C hairpin is replaced by the wild-type sg hairpin (mSg) or the sg hairpin of the revertant (mR). The CG base pairs that close the trinucleotide AUA loop in constructs mWtC and mSg were disrupted in constructs mCdis and mSgdis, respectively, and were restored by complementary mutations in mCres and mSgres, respectively. **C**: Gel electrophoretic analysis of RNA products synthesized by the RdRp in in vitro assays with the template RNAs shown in **A**. The relative activity levels at the bottom of the panel represent the average of three independent experiments; template activity of mWTC was taken as 100%. The standard error of the mean (SEM) is indicated.

lane 9). This indicates that sg transcription by mutant sgC starts at nt C-2. A start at C-2 means that the transcripts of mutant sgC and its derivatives sgCres and sgCΔ are 2 nt longer than the sgWT transcript. This is in agreement with the differences in migration rate seen in Figure 4B. Moreover, the results demonstrate that the four base pairs below the bulge in the stem-loop C hairpin of sgC do not contribute to promoter activity.

The sg hairpin can replace stem-loop C in the BMV minus-strand promoter

Figure 5A shows the model for the RNA secondary structure of the 3′ terminal 171 nt of the 3′ UTR of BMV genomic RNA 3 (adapted from Felden et al., 1994). Stem-loops A, B, C, D, and E constitute the tRNA-like structure. It should be noted that in the minus-strand promoter, transcription initiates 55 nt downstream (or 3′) of the boxed region of stem-loop C at the 3′ end of the genomic RNA (indicated by the arrow), whereas in construct sgC (Fig. 4A) transcription is initiated 9 nt upstream (or 5′) of this boxed region. To analyze the role of the CG base pair that closes the AUA triloop of stem-loop C in minus-strand promoter activity of the 173-nt RNA fragment (171 viral and 2 nonviral nucleotides), this base pair was disrupted in mutant mCdis and restored by a complementing mutation in mCres (Fig. 5B). When the promoter activity of the wild-type fragment (mWtC; Fig. 5C, lane 1) is taken as 100%, disruption of the CG base pair caused a drop in activity to 8% (Fig. 5C, lane 2) whereas the complementing mutation restored activity to 45% (Fig. 5C, lane 3).

Next, we analyzed whether the sg hairpin was functionally equivalent to stem-loop C in minus-strand promoter activity. The boxed region of stem-loop C in the 173-nt fragment was replaced by the wild-type sg hairpin (mutant mSg) or the revertant sg hairpin (mutant mR). To analyze a possible role in promoter activity of the pseudo triloop in mutant mSg, the transloop 5′C_1G_5 base pair was disrupted in mutant mSgdis and restored in mutant mSgres (see Fig. 5B). Previously, we have shown that disruption of the transloop base pair can induce the formation of an alternative hairpin structure (Haasnoot et al., 2000). To prevent this alternative base pairing, the stem of the sg hairpin in constructs mSg, mSgdis, and mSgres was stabilized by mutating of U-21 into C (bold italic in Fig. 5B, panels mSg, mSgdis, and mSgres). This mutation of U-21 does not affect sg promoter activity (Haasnoot et al., 2000). The promoter activity of the 173-nt-long mutant minus-strand promoter transcripts was assayed in an in vitro RdRp assay. The activity of the wild-type promoter (mWtC) in this experiment is shown in lane 4 of Figure 5C and was taken as 100%. Replacement of the boxed region of stem-loop C by the revertant sg hairpin (mR) resulted in a drop in promoter activity to 55% (Fig. 5C, lane 5) whereas replacement by the wild-type sg hairpin (mSg) resulted in a decrease of the activity to 10% (Fig. 5C, lane 6). Disruption of the pseudo triloop by mutation of C-13 in the wild-type sg hairpin to G (mSgdis) further decreased promoter activity to 5% (Fig. 5C, lane 7). A compensating mutation of G-17 into C (mSgres) restored base pairing and restored promoter activity to a level of 10% (Fig. 5C, lane 8). When the 3′ terminal transcription initiation site ACCA3′ was mutated into AGGA3′, no products were synthesized in the RdRp assay (result not shown). This is in line with the notion that minus-strand synthesis initiates at the 3′ proximal C-residue in the 3′ terminal CCA sequence (Chapman & Kao, 1999). Together, the results demonstrate that the sg promoter hairpin can functionally replace stem-loop C in the minus-strand promoter although this hairpin is less efficient in promoting transcription. The RdRp appears to recognize preferentially the AUA loop in both the sg promoter hairpin and the minus-strand core promoter stem-loop C.

Similarities between the BMV sg hairpin, the IRE, and other RNA structures

We noticed that the pseudo triloop of the BMV sg hairpin is structurally very similar to the loop of the iron-responsive elements (Fig. 6). These RNA structures are found at the 5′ and 3′ ends of mRNAs encoding

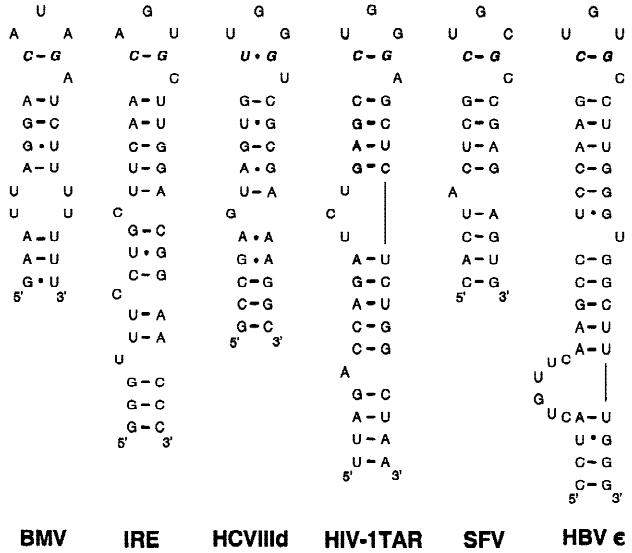

FIGURE 6. Pseudo triloop motifs formed by transloop 5′C_1G_5 base pairing (in bold italics) in the hexanucleotide loops of several secondary RNA structures that are involved in specific protein binding. BMV: Brome mosaic virus subgenomic promoter; IRE: iron-responsive element in human ferritin heavy chain mRNA; HCVIIId: domain IIId of the internal ribosome entry site of Hepatitis C virus; HIV-1 TAR: Transactivational response element of Human immunodeficiency virus 1; SFV: 5′ terminal hairpin of R-U5 of Simian foamy virus; HBV ϵ: encapsidation signal ϵ of Hepatitis B virus. Proteins binding to these structures and the role of the transloop base pair in protein binding are discussed in the text.

proteins involved in iron and oxidative metabolism in animals, and inhibit translation of the messenger by binding of iron regulatory proteins (IRPs) 1 or 2 in the absence of iron (Wang et al., 1990; Harrell et al., 1991; Klausner et al., 1993; Ke et al., 1998; Theil & Eisenstein, 2000). In the IRE, formation of the pseudo triloop by transloop base pairing has also been shown to be essential for its function (Sierzputowska-Gracz et al., 1995; Ke et al., 2000). NMR analysis of the human ferritin heavy chain IRE showed flipping-out of the 3′ bulged C and a compact structure of the loop as a result of stacking residues (Laing & Hall, 1996; Addess et al., 1997). In one-dimensional imino proton spectra of this IRE, a large upfield shift was observed for the transloop imino proton resonance, similar to the signal corresponding to G9 imino proton of the BMV transloop base pair (Fig. 2). As illustrated in Figure 6, putative hexanucleotide loops converted into a pseudo trinucleotide loop by a transloop base pair can also be found in the loop of the Human immunodeficiency virus type 1 (HIV-1) *trans*-activation response element (TAR; Critchley et al., 1993), the encapsidation signal ϵ of Hepatitis B virus (HBV; Knaus & Nassal, 1993; Polack & Ganem, 1993), domain IIId of the internal ribosomal entry site of Hepatitis C virus (HCV; Klinck et al., 2000; Lukavsky et al., 2000) and the 5′ terminal hairpin of R-U5 of Simian foamy virus type 1 (SFV-1; Park & Mergia, 2000). The similarities between the hexanucleotide loops with transloop base pairs shown in Figure 6 suggest that this type of loop structure is a general RNA motif for protein binding.

DISCUSSION

Base pairing in the BMV sg promoter hairpin

It has been well established that RNA secondary structures such as hairpins, hairpin loops, bulges, and internal loops can be involved in protein binding. Based on computer modeling studies, Jaspars (1998) proposed that sg promoters of many viruses from the family *Bromoviridae* would contain a hairpin structure. For two viruses within this family, AMV and Cucumber mosaic virus (CMV), it has been confirmed experimentally that the predicted hairpin structures in these promoters are required for sg transcription (Chen et al., 2000; Haasnoot et al., 2000). In the BMV sg promoter, a stable hairpin could not be predicted by computer modeling, and BMV sg transcription was proposed to take place by sequence-specific recognition of the four contact nucleotides G-17, A-14, C-13, and G-11 (relative to the +1 transcription initiation site; Siegel et al., 1997). Previously, we reported evidence that formation of a pseudo triloop by base pairing between nt C-13 and G-17 is required for BMV sg promoter activity. This structure was found to be conserved in the closely related Cowpea chlorotic mottle virus (CCMV), and was proposed to be the primary recognition site for the RdRp (Haasnoot et al., 2000). In the present study, we used native gel electrophoresis, RNAse T1 structure probing, and NMR spectroscopy to study the BMV sg promoter hairpin. Evidence was obtained that the transloop base pair C-13/G-17 can exist at room temperature in the absence of any protein and is not induced by interaction of the RNA with the RdRp. NMR spectroscopy of the BMV sg promoter hairpin was consistent with the formation of all other proposed base pairs in the absence of BMV RdRp. In addition, in vitro replication assays showed that the lower base pairs (nt −10/−21 and −11/−20) in the BMV sg hairpin contributed to promoter activity, although disruption of a single base pair did not completely abolish sg RNA synthesis. Also for the AMV sg hairpin, it was found that the 5′ CG base pair that closes the trinucleotide 5′ AAU loop is essential for promoter activity, whereas disruption of a single base pair in other parts of the stem was tolerated (Haasnoot et al., 2000). We propose that the BMV pseudo triloop exists in the absence of the RdRp and is an essential element for sg promoter recognition. It cannot be excluded that after binding of the RdRp, the secondary structure of the sg promoter is further stabilized.

A detailed mapping of BMV and CCMV sg promoters made Kao and coworkers favor a sequence-specific rather than a structure-specific recognition of the bromovirus sg promoters (Adkins et al., 1997; Siegel et al., 1997; Adkins & Kao, 1998). These authors made mutations in the BMV −20/+13 and CCMV −20/+11 sg promoters. The observation that mutation of C-20 to G could compensate for the effect of mutation of G-11 to C in the BMV sg promoter made Adkins and Kao (1998) conclude that G-11 and C-20 function together to form a local RNA structure required for promoter recognition. In agreement with this result, the G-20 mutation in our −25/+13 promoter transcript reduced promoter activity to 14%, whereas the compensating mutation in the C-11/G-20 double mutant increased activity to 86% (Fig. 3). Previously, we have shown that a reduction in promoter activity caused by mutation of C-13 into G or G-17 into C could be compensated by combining the two mutations to restore base pairing (Haasnoot et al., 2000). Together, the data indicate that of the 4 nt implicated in sequence-specific contacts, three (G-11, C-13, and G-17) can be mutated without loss of promoter activity as long as the base pairs −11/−20 and −13/−17 are maintained. Our BMV transcript of nucleotides −25/+19 allows the formation of two base pairs (−9/−22 and −10/−21) that are absent in the −20/+13 transcript used by Kao and coworkers. We did not analyze a possible contribution of base pair A-9/U-22 to promoter activity. Disruption of the G-10/U-21 base pair reduced promoter activity to 42%, whereas replacement by a C-10/G-21 base pair increased activ-

ity to 203% (Fig. 3). Our conclusion that this base pair is not essential but contributes to promoter activity differs from the finding of Adkins et al. (1997) that U-21 is dispensable for activity.

Mutation of nucleotides $C_{-20}U_{-19}A_{-18}$ to $G_{-20}A_{-19}U_{-18}$ reduced BMV sg promoter activity to 53% (Siegel et al., 1997). In our model, this mutation would leave a stem of two base pairs (C-13/G-17 and A-12/U-18) to form the triloop. Deletion of nucleotides $C_{-20}U_{-19}A_{-18}$ from the BMV $-20/+13$ transcript reduced promoter activity to 6% although all nucleotides implicated in sequence-specific contacts with the RdRp are present in this transcript (Adkins et al., 1997). The requirement of these three nucleotides for promoter activity is consistent with the proposed role of C-20 and U-19 in base pair formation. It is currently difficult to explain the 172% activity reported for the BMV G-20 mutant (Adkins & Kao, 1998) by a structure-specific recognition of the sg promoter by the BMV RdRp. In our study, the G-20 mutant showed an sg promoter activity of 14% (Fig. 3). The difference between the results may be due to the differences in length of the sg promoter fragments used. However, the viability of the revertant isolated by Smirnyagina et al. (1994) and the sg promoter activity of our construct sgC (Fig. 4) demonstrate that BMV RdRp can recognize a stable hairpin in the sg promoter in vivo and in vitro.

The functional equivalence of the BMV sg hairpin and stem-loop C

Replacement of the wild-type BMV sg promoter hairpin by the hairpin of the second-site revertant isolated by Smirnyagina et al. (1994) (sgR), or the stem-loop C hairpin (sgC) yielded functional templates. Transcription directed by the sgC chimera initiated 2 nt upstream of the wild-type initiation site. This may reflect the slightly larger distance between the top of the stem-loop C hairpin and authentic initiation site in the sgC construct. It has been shown that insertion of nucleotides between positions -4 and -7 of the BMV sg promoter can result in a shift of the site of transcription initiation (Stawicki & Kao, 1999). Sg promoter activity of constructs sgR and sgC was severalfold higher than that of the wild-type sg promoter. The two hairpins within these constructs are considerably more stable than the wild-type hairpin and may generate an AUA triloop that is apparently recognized by the RdRp with greater efficiency. However, the BMV core promoter that was assayed in our experiments did not contain the full 3′ flanking poly(U) tract that enhances the activity of this core promoter (French & Ahlquist, 1987; Marsh et al., 1988; Adkins et al., 1997). The relatively strong sg hairpin structure of the revertant isolated by Smirnyagina et al. (1994) probably compensated for the loss of the poly(U) tract by this revertant. Within the family *Bromoviridae*, the sg promoter hairpins of AMV and ilarviruses are not flanked by a 3′ terminal poly(U) tract and the sg hairpins of these viruses are more stable than the BMV sg hairpin (Jaspars, 1998; Haasnoot et al., 2000). It has been suggested that the poly(U) tract may interact with a host factor to stimulate the formation of an efficient recognition site for the RdRp (Adkins et al., 1997). Alternatively, protein–protein interactions between the putative host factor and RdRp, or a direct interaction between the RdRp and the poly(U) tract may stabilize the initiation complex.

Similar to the revertant hairpin in the sg promoter, the stem-loop C hairpin in the minus-strand promoter functions independently of a poly(U) tract. Replacement of the stem-loop C hairpin in the minus-strand promoter by the revertant sg hairpin resulted in a twofold drop in promoter activity whereas replacement by the wild-type BMV sg hairpin resulted in a10-fold drop in promoter activity. Again, this may reflect the dependency of the wild-type sg hairpin on the poly(U) enhancer. However, the residual activity of mSg is apparently still dependent on the formation of the pseudo triloop as disruption resulted in a further decrease of activity, whereas restoring base pairing in mSgres (Fig. 5) restored promoter activity to 10%.

Stem-loop C is the primary element that is recognized by the RdRp in the minus-strand promoter in vitro (Dreher & Hall, 1988; Chapman & Kao, 1999; Kim et al., 2000). The 5′ A-residues in the triloop of both the BMV sg hairpin and stem-loop C have been shown to be essential for the synthesis in vitro of sg and minus-strand RNA, respectively (Siegel et al., 1997; Adkins & Kao, 1998; Chapman & Kao, 1999; Kim et al., 2000). Analysis of the three-dimensional structure of the stem-loop C triloop by NMR revealed that the 5′ A-residue is exposed to the solvent in a so-called clamped adenine motif and free to interact with the RdRp (Kim et al., 2000; Kim & Tinoco, 2001). The 5′ A-residue in the triloop of the sg hairpin is likely to fulfill a similar function. Although it seems obvious that a viral replicase would recognize a common motif within its various viral promoter sequences with which it interacts, only few such similarities have been identified until now. Here we clearly show that in BMV, the AUA triloop motif represents a common RdRp recognition site, which is required for both sg and minus-strand RNA synthesis. Similarly, the stem-loop structures required for CMV sg promoter and minus-strand promoter activity (Chen et al., 2000; Sivakumaran et al., 2000) may be equivalent in RdRp recognition.

Although our experiments indicate that the sg hairpin and stem-loop C have similar functions in RdRp recognition, the sites of transcription initiation in the sg and minus-strand promoter are rather different. In the sg promoter, initiation occurs about 9 nt upstream (or 5′) of the sg hairpin whereas in the minus-strand promoter, initiation occurs 55 nt downstream (or 3′) of the

stem-loop C hairpin. We propose that the additional RNA sequence elements of the minus-strand promoter play a role in the positioning of the 3′ end of the genomic RNA into the active center of the RdRp.

The pseudo triloop, a novel RNA motif involved in protein binding

One of the most striking features of the BMV sg promoter hairpin is its similarity with the IREs and several other RNA structures that are involved in protein binding. To our knowledge, the BMV sg hairpin was the first viral RNA sequence with protein-binding activity that was found to contain a functional pseudo triloop motif like the IRE (Haasnoot et al., 2000). Disruption of the pseudo triloop in the IRE disrupts protein binding and destabilizes the hairpin structure, resulting in a 10 °C decrease in melting temperature (Sierzputowska-Gracz et al., 1995; Ke et al., 2000). Furthermore, RNA melting experiments revealed that the IRE loop confers exceptional stability to the stem-loop structure, comparable to the stabilization of hairpins by the tetra loops GNRA and UNCG and by the UU-loop (Dale et al., 2000). Comparison of a number of IREs in cellular mRNAs revealed the consensus sequence $5'C_1A_2G_3U_4G_5X_6$, in which the bulged X_6 can be either A, C, or U, but not G (Klausner et al., 1993). Deletion of the 3′ bulged nucleotide resulted in a 80-fold lower affinity for the IRP whereas deletion of other nucleotides from the consensus sequence reduced this affinity 102- to 654-fold (Jaffrey et al., 1993). Mutation of a bulged C-residue of the IRE to an A-residue resulted in an increase of the melting temperature (Dale et al., 2000). Similarly, the bulged A-residue in the BMV sg promoter may contribute to the stability of the hairpin.

The pseudo triloop of the wild-type BMV sg promoter hairpin can be replaced by the regular AUA triloop of the sg revertant sgR and mutant sgC, which are both efficiently recognized by RdRp in vitro. In vivo however, the revertant sg hairpin drives sg transcription at only 35% of the wild-type level (Smirnyagina et al., 1994). This indicates that the pseudo triloop motif in combination with the poly(U) tract is favored above a regular AUA triloop. Therefore, we propose that in the wild-type BMV sg promoter, the pseudo triloop motif with the bulged A-residue acts in concert with the poly(U) tract to modulate promoter strength or the specificity of the interaction between promoter and RdRp.

Recent evidence indicates that pseudo triloop motifs (hexanucleotide loops with a potential transloop base pair between nt 1 and 5) may represent RNA structures that are frequently involved in protein binding. Transactivation of HIV-1 transcription involves binding of cyclin T1 to the TAR loop (Garber et al., 1998; Wei et al., 1998; Zhang et al., 2000). A resemblance between the TAR and IRE loops was first noted by Henderson et al. (1994). However, studies on the structure of the TAR loop yielded contradictory results. Data obtained by NMR spectroscopy favored a flexible loop structure whereas enzymatic structure probing suggested a compact loop structure that is compatible with a potential transloop $5'C_1G_5$ base pair and formation of the pseudo triloop (Colvin & Garcia-Blanco, 1992; Colvin et al., 1993; Critchley et al., 1993; Jaeger & Tinoco, 1993; Long & Crothers, 1999). Interestingly, a phylogenetic analysis of TAR elements in various strains of HIV and Simian immunodeficiency virus (SIV) clearly supports the existence of a transloop base pair in the TAR loop (P.C.J. Haasnoot, B. Berkhout, & J.F. Bol, unpubl. results). In HBV, the loop sequence of the encapsidation signal ϵ has been shown to interact with the viral replicase protein P (Tavis et al., 1994; Nassal & Rieger, 1996). Although Knaus and Nassal (1993) did not propose a pseudo triloop motif in the encapsidation signal ϵ, their enzymatic structure probing data support the occurrence of a transloop $5'C_1G_5$ base pair in this hexanucleotide loop. The apical loop of the IIId domain of in the 5′UTR of HCV has been shown to interact with the ribosomal protein S9, which is required for IRES-directed translation, and the viral core protein (Odreman-Macchioli et al., 2000; Tanaka et al., 2000). Recently, NMR studies and enzymatic structure probing demonstrated that the hexanucleotide loop of subdomain IIId in the 5′ UTR of HCV adopts a pseudo triloop structure by formation of a $5'U_1G_5$ transloop base pair (Klinck et al., 2000).

The similarities between these diverse RNA structures and their specific interactions with proteins suggest that pseudo triloop motifs provide convenient targets for various RNA–protein interactions, whereby the sequence of the triloop part probably ensures the specificity. As RdRps of RNA viruses contain many conserved features (O'Reilly & Kao, 1998), it will be interesting to see to what extent pseudo triloop motifs are involved in the binding of these RdRps to their cognate viral RNAs.

MATERIALS AND METHODS

Native gel electrophoresis and RNase T1 probing of RNA oligos

Synthetic RNA oligoribonucleotides WT (5′AGGACAUAG AUCUU) and A-13 (5′AGGA*A*AUAGAUCUU) were 5′ labeled with γ-^{32}P-ATP and T4 polynucleotide kinase. Equal amounts of labeled WT and A-13 oligoribonucleotides were run at room temperature on a denaturing 20% polyacrylamide gel containing 8 M urea in TBE buffer, using a formamide-based loading buffer, or on a 12% nondenaturing polyacrylamide gel in TB buffer at a room temperature of 26 °C using a glycerol-based loading buffer. RNA fragments were visualized by autoradiography. For structure probing, 0.4 μg labeled oligoribonucleotide plus 5 μg tRNA was di-

gested with 1×10^{-3} to 10×10^{-3} U RNAse T1 in HMK buffer (70 mM HEPES-KOH, pH 7.8, 10 mM $MgCl_2$, and 270 mM KCl) in total volume of 7.5 μL for 15 min on ice, and directly run on a 20% polyacrylamide gel containing 8 M urea. RNA fragments were visualized by autoradiography and quantified with a PhosphorImager.

NMR analysis

One-dimensional imino proton NMR spectra for the RNA hairpins WT and A-13 were recorded at 277 K on a 600-MHz Bruker NMR spectrometer, using a watergate pulse sequence for water suppression (Piotto et al., 1992). The 14-nt RNA oligoribonucleotides were dissolved in 400 μL to a concentration of 0.2 mM RNA in 10%/90% D_2O/H_2O, 30 mM NaCl, 10 mM Na_2PO_4, pH 5.8. For each oligonucleotide 1,000 scans were recorded. The NMR data were processed on a SGI workstation using XWIN-NMR2.6 software.

Preparation of template RNAs

Template RNAs with BMV sgp sequences were transcribed from DNA fragments amplified by PCR from the BMV cDNA 3 clone pB3TP7 (Janda et al., 1987) using proofreading Vent DNA polymerase (New England Biolabs). The sgWt sequence was amplified with a downstream primer (primer BT7+17) containing the T7 RNA polymerase promoter fused to the sequence complementary to nt +17 to −4 (taking the transcription start site of RNA 4 as +1) and an upstream primer corresponding to nt −25 to +11. Mutant BMV sgp sequences shown in Figure 4 were amplified by PCR with upstream primers containing the mutations indicated in the text. Similarly, the chimeric promoter constructs shown in Figure 5 were amplified by PCR with the downstream primer BT7+17 and upstream primers corresponding to the indicated sequences.

Templates with BMV minus-strand promoter sequences were transcribed from DNA fragments amplified by two rounds of PCR from the BMV cDNA 3 clone pB3TP using proofreading Vent DNA polymerase (New England Biolabs). The wild-type minus-strand promoter sequence shown in Figure 5 was amplified with an upstream primer containing the T7 RNA polymerase promoter fused to the sequence complementary to nt +153 to +171 (primer T7BM) taking the 3′ terminal nucleotide of RNA 3 as +1, and a downstream primer corresponding to nt +1 to +25 (primer BM3). Mutant minus-strand promoters shown in Figure 5 were generated by fusion PCR of two separate PCR fragments containing the desired mutations. The 5′ half was generated by PCR using primer T7B and antisense primers containing the desired mutations fused to priming sequences corresponding to nt +76 to +94. The 3′ half was generated by using primer BM3 and sense primers containing the desired mutations fused to priming sequences corresponding to nt +56 to +38. The PCR products corresponding to the 5′ and 3′ halves of the BMV 3′ UTR were isolated from gel and fused in a second round of PCR using the T7B and BM3 primers. For the amplification of templates in which the transcription initiation site 5′ ACCA is mutated to 5′ A*GG*A, primer B+1CC with the corresponding mutation was used instead of primer BM3.

Transcripts made with T7 RNA polymerase were purified by extraction with phenol/chloroform, precipitated two times with isopropanol in the presence of ammonium acetate, analyzed on ethidium bromide stained agarose gels, and quantified by UV absorbance.

RdRp assay

BMV RdRp was kindly provided by the late Dr. E.M.J. Jaspars. The enzyme was isolated from BMV-infected barley leaves, and purified as described by Bujarski et al. (1982) through sucrose gradient centrifugation, using dodecyl-β-D-maltoside as detergent. Five microliters of the sucrose gradient fraction was treated with micrococcal nuclease and used in the RdRp assay. The various BMV promoter fragments described here were all tested at least three times and the autoradiographs shown are representative for these assays. In vitro RNA synthesis was performed in a 50-μL mixture containing 10 pmol template RNA, 5 μL BMV RdRp, 50 mM Tris-HCl, pH 8.2, 10 mM $MgCl_2$, 10 mM DTT, 1 mM each ATP, GTP, and CTP, 10 μM UTP, and 5 μCi [α-^{32}P]UTP (400 Ci/mmol). The mixtures were incubated at 28 °C for 60 min.

Labeled RNA products were purified by phenol/chloroform extraction and isopropanol precipitation, in the presence of 0.6 M ammoniumacetate and were run on a 20% or 10% polyacrylamide gel containing 8 M urea in TBE buffer. The RNAs were visualized by autoradiography and quantified with a PhosphorImager.

ACKNOWLEDGMENTS

Thanks are due to Mrs. C.J. Houwing and the late Dr. E.M.J. Jaspars for providing the BMV RdRp preparation. This work was supported in part by the Foundation for Chemical Sciences (CW) of the Netherlands Organization for Scientific Research (NWO).

Received June 18, 2001; revised manuscript received October 25, 2001

REFERENCES

Addess KJ, Basilion JP, Klausner RD, Roualt TA, Pardi A. 1997. Structure and dynamics of the iron responsive element RNA: Implications for binding of the RNA by iron regulatory binding proteins. *J Mol Biol 274*:72–83.

Adkins S, Kao CC. 1998. Subgenomic RNA promoters dictate the mode of recognition by bromoviral RNA-dependent RNA polymerases. *Virology 252*:1–8.

Adkins S, Siegel RW, Sun J-H, Kao CC. 1997. Minimal templates directing accurate initiation of subgenomic RNA synthesis in vitro by the brome mosaic RNA-dependent RNA polymerase. *RNA 3*:634–647.

Bol JF. 1999. Alfalfa mosaic virus and ilarviruses: Involvement of coat protein in multiple steps of the replication cycle. *J Gen Virol 80*:1089–1102.

Buck KW. 1996. Comparison of the replication of positive-stranded RNA viruses of plants and animals. *Adv Virus Res 47*:159–251.

Bujarski JJ, Hardy SF, Miller WA, Hall TC. 1982. Use of dodecyl-β-D-maltoside in the purification and stabilization of RNA polymerase from brome mosaic virus-infected barley. *Virology 119*:465–473.

Carpenter CD, Simon AE. 1998. Analysis of sequences and predicted structures required for viral satellite RNA accumulation by in vivo genetic selection. *Nucleic Acids Res 26*:2426–2432.

Chapman MR, Kao CC. 1999. A minimal RNA promoter for minus-strand RNA synthesis by the brome mosaic virus polymerase complex. *J Mol Biol 286*:709–720.

Chen MH, Roossinck MJ, Kao CC. 2000. Efficient and specific initiation of subgenomic RNA synthesis by cucumber mosaic virus replicase in vitro requires an upstream RNA stem-loop. *J Virol 74*:11201–11209.

Colvin RA, Garcia-Blanco MA. 1992. Unusual structure of the human immunodeficiency virus type 1 transactivation response element. *J Virol 66*:930–935.

Colvin RA, White SW, Garcia-Blanco MA, Hoffman DW. 1993. Structural features of an RNA containing the CUGGGA loop of the human immunodeficiency virus type 1 transactivation response element. *Biochemistry 32*:1105–1112.

Critchley AD, Haneef I, Cousens DJ, Stockley PG. 1993. Modeling and solution structure of the HIV-1 TAR stem-loop. *J Mol Graphics 11*:92–97.

Dale T, Smith R, Serra MJ. 2000. A test of the model to predict unusually stable RNA hairpin loop stability. *RNA 6*:608–615.

Dreher TW. 1999. Functions of the 3′-untranslated regions of positive strand RNA viral genomes. *Annu Rev Phytopathol 37*:151–174.

Dreher TW, Hall TC. 1988. Mutational analysis of the tRNA mimicry of brome mosaic virus RNA. Sequence and structural requirements for aminoacylation and 3′ adenylation. *J Mol Biol 201*:41–55.

Duggal R, Lahser F, Hall T. 1994. *Cis*-acting sequences in the replication of plant viruses with plus-sense RNA genomes. *Annu Rev Phytopathol 32*:287–309.

Felden B, Florentz C, Giegé R, Westhof E. 1994. Solution structure of the 3′ end of Brome mosaic virus genomic RNAs. *J Mol Biol 253*:508–531.

French R, Alquist P. 1987. Intercistronic as well as terminal sequences are required for efficient amplification of brome mosaic virus RNA 3. *J Virol 61*:1457–1465.

French R, Alquist P. 1988. Characterization and engineering of sequences controlling in vivo synthesis of brome mosaic virus subgenomic RNA. *J Virol 62*:2411–2420.

Garber ME, Wei P, KewalRamani VN, Mayall TP, Herrmann CH, Rice AP, Littman DR, Jones KA. 1998. The interaction between HIV-1 Tat and human cyclin T1 requires zinc and a critical cysteine residue that is not conserved in the murine CycT1 protein. *Genes & Dev 12*:3512–3527.

Haasnoot PCJ, Brederode FTh, Olsthoorn RCL, Bol JF. 2000. A conserved hairpin structure in Alfamovirus and Bromovirus subgenomic promoters is required for efficient RNA synthesis in vitro. *RNA 6*:708–716.

Harrell CM, Mckenzie AR, Patino MM, Walden WE, Theil EC. 1991. Ferritin mRNA: Interactions of the iron regulatory element with translational regulator protein P-90 and the effect on base-paired flanking regions. *Proc Natl Acad Sci USA 88*:4166–4170.

Henderson BR, Menotti E, Bonnard C, Kuhn LC. 1994. Optimal sequence and structure of iron-responsive elements. Selection of RNA stem-loops with high affinity for iron regulatory factor. *J Biol Chem 269*:17481–17489.

Jaeger JA, Tinoco I. 1993. An NMR study of the HIV-1 TAR element hairpin. *Biochemistry 32*:12522–12530.

Jaffrey SR, Haile DJ, Klausner RD, Harford JB. 1993. The interaction between the iron-responsive element binding protein and its cognate RNA is highly dependent upon both RNA sequence and structure. *Nucleic Acids Res 21*:4627–4631.

Janda M, French R, Ahlquist P. 1987. High efficiency T7 polymerase synthesis of infectious RNA from cloned brome mosaic virus cDNA and effects of 5′ extensions of transcript infectivity. *Virology 158*:259–262.

Jaspars EMJ. 1998. A core promoter hairpin is essential for subgenomic RNA synthesis in alfalfa mosaic alfamo virus and is conserved in other *Bromoviridae*. *Virus Genes 17*:233–242.

Ke Y, Sierzputowska-Gracz H, Gdaniec Z, Theil EC. 2000. Internal loop/bulge and hairpin loop of the iron-responsive element of the ferritin mRNA contribute to maximal iron regulatory protein 2 binding and transcriptional regulation in the iso-iron-responsive element/iso-iron regulatory protein family. *Biochemistry 39*:6235–6242.

Ke Y, Wu J, Leibold EA, Walden WE, Theil EC. 1998. Loops and bulge/loops in iron-responsive element isofroms influence iron regulatory protein binding. *J Biol Chem 273*:23637–23640.

Kim CH, Kao CC, Tinoco I. 2000. RNA motifs that determine specificity between a viral replicase and its promoter. *Nature Struct Biol 7*:415–423.

Kim CH, Tinoco I. 2001. Structural and thermodynamic studies on mutant RNA motifs that impair the specificity between a viral replicase and its promoter. *J Mol Biol 307*:827–839.

Klausner RD, Rouault TA, Harford JB. 1993. Regulating the fate of mRNA: The control of cellular iron metabolism. *Cell 72*:19–28.

Klinck R, Westhof E, Walker S, Afshar M, Collier A, Aboul-Ela F. 2000. A potential RNA drug target in the hepatitis C virus internal ribosomal entry site. *RNA 6*:1423–1431.

Knaus T, Nassal M. 1993. The encapsidation signal on the hepatitis B virus RNA pregenome forms a stem-loop structure that is critical for its function. *Nucleic Acids Res 21*:3967–3975.

Lai MM, Cavanagh D. 1997. The molecular biology of coronaviruses. *Adv Virus Res 48*:1–100.

Laing LG, Hall KB. 1996. A model of the iron responsive element RNA hairpin loop structure determined from NMR and thermodynamic data. *Biochemistry 35*:13586–13596.

Long KS, Crothers DM. 1999. Characterization of the solution conformations of unbound and at peptide-bound forms of HIV-1 TAR RNA. *Biochemistry 38*:10059–10069.

Lukavsky PJ, Otto GA, Lancaster AM, Sarnow P, Puglisi JD. 2000. Structures of two RNA domains essential for hepatitis C virus internal ribosome entry site function. *Nature Struct Biol 7*:1105–1110.

Marsh LE, Dreher TW, Hall TC. 1988. Mutational analysis of the core and modulator sequences of BMV RNA 3 subgenomic promoter. *Nucleic Acids Res 16*:981–995.

Miller WA, Dreher TW, Hall TC. 1985. Synthesis of brome mosaic virus subgenomic RNA in vitro by internal initiation on (−) sense genomic RNA. *Nature 313*:68–70.

Miller WA, Koev G. 2000. Synthesis of subgenomic RNAs by positive-strand RNA viruses. *Virology 273*:1–8.

Nassal M, Rieger A. 1996. A bulged region of the hepatitis B virus RNA encapsidation signal contains the replication origin for discontinuous first-strand DNA synthesis. *J Virol 70*:2764–2773.

Odreman-Macchioli FE, Tisminetzky AG, Zottie M, Baralle FE, Buratti E. 2000. Influence of correct secondary and tertiary RNA folding on the binding of cellular factors to the HCV IRES. *Nucleic Acids Res 28*:875–885.

Oh JW, Sheu GT, Lai MM. 2000. Template requirement and initiation site selection by hepatitis C virus polymerase on a minimal viral RNA template. *J Biol Chem 275*:17710–17717.

Olsthoorn RCL, Mertens S, Brederode FTh, Bol JF. 1999. A conformational switch at the 3′ end of a plant virus RNA regulates viral replication. *EMBO J 18*:4856–4864.

O'Reilly EK, Kao CC. 1998. Analysis of RNA-dependent RNA polymerase structure and function as guided by known polymerase structures and computer predictions of secondary structure. *Virology 252*:287–303.

Park J, Mergia A. 2000. Mutational analysis of the 5′ leader region of the simian foamy virus type 1. *Virology 274*:203–212.

Piotto M, Saudek V, Sklenar V. 1992. Gradient-tailored excitation for single-quantum NMR spectroscopy of aqueous solutions. *J Biomol NMR 2*:661–665.

Polack JR, Ganem D. 1993. An RNA stem-loop structure directs hepatitis B virus genomic RNA encapsidation. *J Virol 67*:3254–3263.

Rao ALN, Hall TC. 1993. Recombination and polymerase error facilitate restoration of infectivity in brome mosaic virus. *J Virol 67*:969–979.

Rybicki EP. 1995. *Bromoviridae*. *Virus Taxonomy. Sixth Report of the International Committee on Taxonomy of Viruses*. Vienna & New York: Springer-Verlag. pp 450–457.

Sawicki SG, Sawicki DL. 1998. A new model for coronavirus transcription. *Adv Exp Med Biol 440*:215–219.

Siegel RW, Adkins S, Kao CC. 1997. Sequence-specific recognition of a subgenomic RNA promoter by a viral RNA polymerase. *Proc Natl Acad Sci USA 94*:11238–11243.

Sierzputowska-Gracz H, Mckenzie RA, Theil EC. 1995. The importance of a single G in the hairpin loop of the iron-responsive element (IRE) in ferritin mRNA for structure: An NMR spectroscopy study. *Nucleic Acids Res 23*:146–153.

Sivakumaran K, Bao Y, Roossinck MJ, Kao CC. 2000. Recognition of the core RNA promoter for minus-strand RNA synthesis by the replicases of brome mosaic virus and cucumber mosaic virus. *J Virol 74*:10323–10331.

Sit TL, Vaewhongs AA, Lommel SA. 1998. RNA-mediated transactivation of transcription from a viral RNA. *Science 281*:829–832.

Smirnyagina E, Hsu YH, Chua N, Ahlquist P. 1994. Second-site mutations in the brome mosaic virus RNA3 intercistronic region partially suppress a defect in coat protein mRNA transcription. *Virology 198*:427–436.

Stawicki SS, Kao CC. 1999. Spatial perturbations within an RNA promoter specifically recognized by a viral RNA-dependent RNA polymerase (RdRp) reveal that RdRp can adjust its promoter binding sites. *J Virol 73*:198–204.

Tanaka Y, Shimoike T, Ishii K, Suzuki R, Suzuki T, Ushijima H, Matsuura Y, Miyamura T. 2000. Selective binding of hepatitis C virus core protein to synthetic oligonucleotides corresponding to the 5′ untranslated region of the viral genome. *Virology 270*:229–236.

Tavis JE, Perri S, Ganem D. 1994. Hepadnavirus reverse transcription initiates within the stem-loop of the RNA packaging signal and employs a novel strand transfer. *J Virol 68*:3536–3543.

Theil EC, Eisenstein RS. 2000. Combinatorial mRNA regulation: Iron-regulatory proteins and iso-iron responsive elements (iso-IREs). *J Biol Chem 275*:40659–40662.

Tsai CH, Cheng CP, Peng CW, Lin BY, Lin NS, Hsu YH. 1999. Sufficient length of a poly(A) tail for the formation of a potential pseudoknot is required for efficient replication of bamboo mosaic potexvirus RNA. *J Virol 73*:2703–2709.

van der Kuyl AC, Langereis K, Houwing CJ, Jaspars EMJ, Bol JF. 1990. *Cis*-acting elements involved in replication of alfalfa mosaic virus RNAs in vitro. *Virology 176*:346–354.

van Marle G, Dobbe JC, Gultyaev AP, Luytjes W, Spaan WJM, Snijder EJ. 1999. Arterivirus discontinuous mRNA transcription is guided by base pairing between sense and antisense transcription regulating sequences. *Proc Natl Acad Sci USA 96*:12056–12061.

Wang J, Bakkers JM, Galama JM, Bruins Slot HJ, Pilipenko EV, Agol VI, Melchers WJ. 1999. Structural requirements of the higher order RNA kissing element in the enteroviral 3′UTR. *Nucleic Acids Res 27*:485–490.

Wang J, Simon AE. 1997. Analysis of the two subgenomic RNA promoters for turnip crinkle virus in vivo and in vitro. *Virology 232*:174–186.

Wang YH, Sczekan SR, Theil EC. 1990. Structure of the 5′ untranslated regulatory region of the ferritin mRNA studied in solution. *Nucleic Acids Res 18*:4463–4469.

Wei P, Garber ME, Fang SM, Fischer WH, Jones KA. 1998. A novel CDK9-associated C-type cyclin interacts directly with HIV-1 Tat and mediates its high-affinity, loop specific binding to TAR RNA. *Cell 92*:451–462.

Zhang J, Tamilarasu N, Hwang S, Garber ME, Huq I, Jones KA, Rana TM. 2000. HIV-1 TAR RNA enhances the interaction between Tat and cyclin T1. *J Biol Chem 275*:34314–34319.